

Output Tracking of an Unmanned Tandem Helicopter Based On Dynamic Augment Method

Chun-hua Hu, Ji-hong Zhu, Xing-li Huang, Jin-chun Hu, and Zeng-qi Sun

Abstract: The unmanned tandem helicopter, which is a MIMO nonlinear system with complexity and inherent instability, exists in unstable zero dynamics. In this paper, approximate linearization is presented to design the controller for output tracking of an unmanned tandem helicopter based on the dynamic augment method, and the simulation results are encouraging.

Keywords: Approximate linearization, dynamic augment, output tracking, unmanned tandem helicopter.

LIST OF SYMBOLS

a_s^f, a_s^r	longitudinal tilt of the tip path plane of the front and rear rotors	\mathbf{v}^b	velocity vector in body coordinates
b_s^f, b_s^r	lateral tilt of the tip path plane of the front and rear rotors	$\alpha_f, \beta_f, \rho_f$	constant parameters
F_x, F_y, F_z	the resultant forces	$\alpha_r, \beta_r, \rho_r$	constant parameters
g	gravitational acceleration	$\delta_c, \delta_e, \delta_a$	collective pitch, longitudinal cyclic pitch and lateral cyclic pitch
m	helicopter total mass	ϕ, θ, ψ	helicopter angular position
I_x, I_y, I_z	fuselage rotational moments of inertia	$\boldsymbol{\omega}^b$	angular velocity of helicopter in body coordinates
I	inertia matrix of helicopter	$\Gamma_x, \Gamma_y, \Gamma_z$	the resultant moments
P	the position vector of helicopter in inertial coordinates	Θ	transform matrix of Euler angles relative to angular velocities in body frame
R	rotation matrix of the body axes relative to the spatial axes		
R_f, M_f, N_f	moments generated by front rotor		
R_r, M_r, N_r	moments generated by rear rotor		
T_f, T_r	thrusts generated by the front and rear rotors		
X_m^f, Y_m^f, Z_m^f	forces generated by front rotor		
X_m^r, Y_m^r, Z_m^r	forces generated by rear rotor		
\mathbf{v}^p	velocity vector in inertial coordinates		

1. INTRODUCTION

Unmanned Helicopters make interesting platforms for UAVs because they give UAVs the ability to take off and land vertically, and to hover. Unmanned helicopters can remove individuals from dull, dirty, and dangerous tasks or allow the conduct of missions having duration beyond a lifespan. But it is also well known that unmanned helicopters are difficult to control. They are complicated systems with severe nonlinear and coupling.

Frank N. Piasecki developed the first tandem helicopter, PV-3. Piasecki's company eventually became the Boeing Vertol Company, with the tandem configuration remaining its basic production type [1]. Now the CH-47, which is the newest tandem helicopter, is the main military conveyance of the American Army.

Generally, the study of helicopters or unmanned helicopters focused on single-rotor helicopters. Few studies have been done to develop controllers for tandem helicopters. NASA started some studies in the 1950s and the flying qualities such as lateral-directional stability, transition and speed stability were

Manuscript received January 2, 2004; revised April 2, 2004; accepted April 3, 2004. Recommended by Editorial Board member Guang-Ren Duan under the direction of Editor Keum-Shik Hong. This work was supported by the National High Technology 863 Plan of China under Grant No. 2002AA756022.

Chun-Hua Hu, Xing-Li Huang, Ji-Hong Zhu, Jin-Chun Hu, and Zeng-Qi Sun are with the State Key Lab of Intelligent Technology and Systems, Department of Computer Science and Technology, Tsinghua University, Beijing 100084, China (e-mail: huchunhua99@mails.tsinghua.edu.cn, {hxl,zjh,kesai}@s1000e.cs.tsinghua.edu.cn, szq-dcs@mail.tsinghua.edu.cn).

investigated in these studies [2-4]. Dzul developed a simple dynamic model for a tandem helicopter close to hover state, and proposed a backstepping control design for output tracking [5]. Rao used the Lagrangian method to model a side-by-side tandem helicopter, and controlled it with feedback design [6]. These studies all focused on manned tandem helicopters.

Nonlinear transformation has been applied to the automatic flight control of helicopters [7,8]. Exact input-output linearization and approximate linearization have also been studied [9,10]. The objects investigated were all single rotor helicopters. In this paper, we investigate the design of output tracking for an unmanned tandem helicopter based on the dynamic augment method.

The paper is organized as follows. In Section 2, we derive a dynamic model of the unmanned tandem helicopter. Output tracking design based on the dynamic augment method is discussed in Section 3. Some simulation results that illustrate the performance of the controller design based on the dynamic augment method are shown in Section 4. Finally, we present the conclusion of this work.

2. DYNAMIC MODEL OF THE UNMANNED TANDEM HELICOPTER

An unmanned tandem helicopter (refer to Fig. 1) is an aircraft that has two rotor systems installed longitudinally at either end of the fuselage. The major differences between tandem rotor helicopters and single main rotor helicopters are that there is no net yaw moment on the helicopter because the torque of the rotors is equal and opposing. The tandem helicopter behaves as if it had a single main rotor with truly decoupled longitudinal and lateral dynamics. Typically, the two rotors have a longitudinal separation of $1.5r$ to $1.8r$ between the shafts, and hence a 20% to 50% overlap of the rotor disks. To minimize the aerodynamic interference created by the operation of the rear rotor in the wake of the front, the rear rotor is elevated on a pylon ($0.3r$ to $0.5r$ above the front rotor). However, the tandem rotor helicopter can still be considered as longitudinal symmetric if ignoring the vertical rotor separation (the rear rotor is elevated above the front rotor), the inertial and aerodynamic effects of the rear rotor pylon, and offset of the helicopter's center of gravity from midway between the rotors. The unmanned tandem helicopter we developed obeys these characteristics. Eight actuators are installed on the unmanned tandem helicopter for flight control, three for front rotor, three for rear rotor, and another two for engines. The actuator for each engine is closely joined with the actuators for collective pitch.

The collective pitch, lateral cyclic pitch and longitudinal

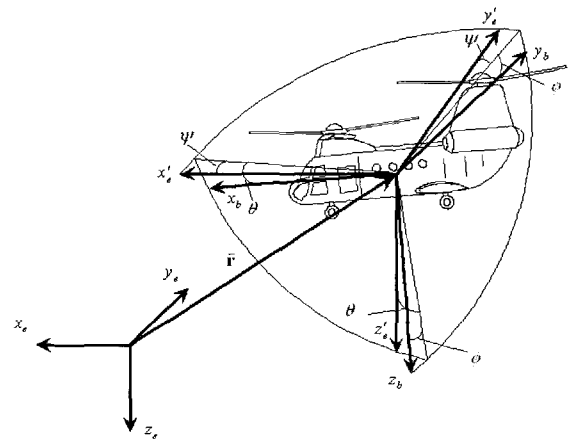


Fig. 1. Unmanned tandem helicopter's configuration with the coordinates defined. The inertial frame is fixed to the ground, and the body frame is fixed to the helicopter.

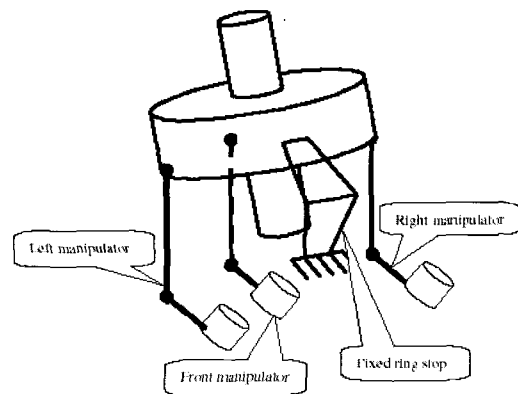


Fig. 2. Manipulator of the rotor.

cyclic pitch are controlled by three actuators for each rotor (refer to Fig. 2). And the relation equation between the output angles of the three actuators $\theta_r, \theta_l, \theta_n$ and the collective pitch δ_c , lateral cyclic pitch δ_a and longitudinal cyclic pitch δ_e is as follows,

$$\begin{bmatrix} \delta_a \\ \delta_e \\ \delta_c \end{bmatrix} = \begin{bmatrix} \frac{n}{2r} & -\frac{n}{2r} & 0 \\ -\frac{n}{r} & -\frac{n}{r} & \frac{2n}{r} \\ \frac{n}{2r_c} & \frac{n}{2r_c} & 0 \end{bmatrix} \begin{bmatrix} \theta_r \\ \theta_l \\ \theta_n \end{bmatrix} + \begin{bmatrix} 0 \\ 0 \\ (l - y_{o_e})/r_c \end{bmatrix}, \quad (1)$$

where n, l are lengths of manipulator's connecting rods, r is radius of fixed ring, o_e is the original point of collective pitch in the shaft, and r_c is the maximum distance of collective pitch in the shaft.

For simplicity, we will present here the dynamic model of the unmanned tandem helicopter in hovering state. The model is proposed using the Newton-Euler method with the following assumptions.

- 1) The front rotor blades are assumed to rotate in an anti-clockwise direction when viewed from above and the rear rotor blades rotate in a clockwise direction.
- 2) The collective pitches of front rotor and rear rotor are equal and the rotation velocity of rotors hold as the same. So the thrusts of two rotors are identical.
- 3) The aerodynamic interference created by the operation of the rear rotor in the wake of the front is ignored.
- 4) The longitudinal cyclic pitches of the two rotors are assumed to be identical.
- 5) It is assumed that the lateral cyclic pitches of the two rotors are controllable. Along with the collective pitch and longitudinal cyclic pitch, these four form the control inputs of the helicopter.

With the assumptions above, we have

$$T_m = T_f = T_r, \quad a_s = a_s^f = a_s^r, \quad (2)$$

and they are related to the collective pitch, longitudinal cyclic pitch and lateral cyclic pitch [11]:

$$T_i = c_1 \delta_c^i + c_3 \delta_c^{i3}, \quad a_s^i = \delta_e^i, \quad b_s^i = \delta_a^i, \quad (3)$$

So the pseudo control input can be reselected as T_m, a_s, b_s^f, b_s^r . The forces and torques generated by the rotors can be written as:

$$\begin{aligned} X_m^i &= T_i \sin a_s, & R_i &= \alpha_i b_s^i - \rho_i \sin a_s, \\ Y_m^i &= T_i \sin b_s^i, & M_i &= \beta_i a_s - \rho_i \sin b_s^i, \\ Z_m^i &= -T_i \cos a_s \cos b_s^i, & N_i &= -\rho_i \cos a_s \cos b_s^i, \end{aligned} \quad (4)$$

where $i = f, r$ in equations (3) and (4).

In hover or forward flight with slow velocity, the velocity is so slow that we can ignore the drag contributed from the fuselage. So resultant force and torque can be written as:

$$\mathbf{F} = \begin{bmatrix} X_m \\ Y_m \\ Z_m \end{bmatrix} + \mathbf{R}^T \begin{bmatrix} 0 \\ 0 \\ mg \end{bmatrix}, \quad (5)$$

$$\mathbf{\Gamma} = \begin{bmatrix} R_m + Y_m^f h_f + Y_m^r h_r \\ M_m - X_m^f h_f - X_m^r h_r - Z_m^f l_f + Z_m^r l_r \\ N_m + Y_m^f l_f - Y_m^r l_r \end{bmatrix}, \quad (6)$$

where

$$\begin{aligned} X_m &= X_m^f + X_m^r, \\ Y_m &= Y_m^f + Y_m^r, \end{aligned} \quad (7)$$

$$\begin{aligned} Z_m &= Z_m^f + Z_m^r, \\ R_m &= R_f + R_r, \\ M_m &= M_f + M_r, \end{aligned} \quad (8)$$

$$N_m = N_f + N_r.$$

And the rotation matrix \mathbf{R} represents the relative orientation between the reference inertial frame and the body frame attached to the unmanned tandem helicopter,

$$\mathbf{R} = \begin{bmatrix} c\psi c\theta & -s\psi c\theta + c\psi s\theta s\phi & s\psi s\theta + c\psi s\theta c\phi \\ s\psi c\theta & c\psi c\theta + s\psi s\theta s\phi & -c\psi s\theta + s\psi s\theta c\phi \\ -s\theta & c\theta s\phi & c\theta c\phi \end{bmatrix} \quad (9)$$

The dynamic equations of the helicopter's motion are significantly simplified by expressing them in body coordinates. In these coordinates, Euler's equations for the rigid body motion of the unmanned tandem helicopter become

$$\begin{aligned} m(\dot{u}^b + w^b q - v^b r) &= F_x, \\ m(\dot{v}^b + u^b r - w^b p) &= F_y, \\ m(\dot{w}^b + v^b p - u^b q) &= F_z, \\ I_x \dot{p} - (I_y - I_z)qr &= \Gamma_x, \\ I_y \dot{q} - (I_z - I_x)rp &= \Gamma_y, \\ I_z \dot{r} - (I_x - I_y)pq &= \Gamma_z, \end{aligned} \quad (10)$$

where $\mathbf{v}^b = (u^b, v^b, w^b)$ is the velocity vector of the helicopter in body coordinates and $\boldsymbol{\omega}^b = (p, q, r)$ is the angular velocity vector of the helicopter in body coordinates.

So the following set of differential equations composes the complete model of the unmanned tandem helicopter.

$$\begin{bmatrix} \dot{p} \\ \dot{q} \\ \dot{r} \end{bmatrix} = \begin{bmatrix} u^p \\ v^p \\ w^p \end{bmatrix}, \quad (11)$$

$$\begin{bmatrix} \dot{u}^p \\ \dot{v}^p \\ \dot{w}^p \end{bmatrix} = \frac{1}{m} \begin{bmatrix} R_{11}X_m + R_{12}Y_m + R_{13}Z_m \\ R_{21}X_m + R_{22}Y_m + R_{23}Z_m \\ R_{31}X_m + R_{32}Y_m + R_{33}Z_m + mg \end{bmatrix}, \quad (12)$$

$$\begin{bmatrix} \dot{\phi} \\ \dot{\theta} \\ \dot{\psi} \end{bmatrix} = \begin{bmatrix} (pc\theta + qs\phi s\theta + rc\phi s\theta) / c\theta \\ qc\phi + rs\phi \\ (qs\phi + rc\phi) / c\theta \end{bmatrix}, \quad (13)$$

$$\begin{bmatrix} \dot{P} \\ \dot{q} \\ \dot{r} \end{bmatrix} = \begin{bmatrix} \frac{1}{I_x} (R_m + Y_m^f h_f + Y_m^r h_r - (I_z - I_y)qr) \\ \frac{1}{I_y} (M_m - X_m^f h_f - X_m^r h_r - Z_m^f l_f + Z_m^r l_r - (I_x - I_z)rp) \\ \frac{1}{I_z} (N_m + Y_m^f l_f - Y_m^r l_r - (I_y - I_x)pq) \end{bmatrix}, \quad (14)$$

where

$$\mathbf{P} = [P_x \quad P_y \quad P_z]^T$$

and

$$\mathbf{v}^p = [u^p \quad v^p \quad w^p]^T$$

are position and velocity in the inertial frame, and

$$\begin{aligned} s\phi &= \sin \phi, & c\phi &= \cos \phi, \\ s\theta &= \sin \theta, & c\theta &= \cos \theta, \end{aligned}$$

R_{ij} represents the element of i^{th} row, j^{th} column in rotation matrix \mathbf{R} .

Define

$$\mathbf{x} = [P_x, P_y, P_z, u, v, w, \phi, \theta, \psi, p, q, r, T_m, a_s, b_{fs}, b_{rs}]^T. \quad (15)$$

Assume that the inputs are derivatives of T_m, a_s, b_{fs}^f and b_{rs}^r , then the state equation can be derived as follows,

$$\dot{\mathbf{x}} = \begin{bmatrix} \mathbf{v}^p \\ \frac{1}{m} \mathbf{R}\mathbf{F} \\ \mathbf{\Theta}\boldsymbol{\omega}^b \\ \mathbf{I}^{-1}(\boldsymbol{\Gamma} - \boldsymbol{\omega}^b \times \mathbf{I}\boldsymbol{\omega}^b) \\ u_1 \\ u_2 \\ u_3 \\ u_4 \end{bmatrix}, \quad (16)$$

where $\mathbf{\Theta}$ is the transform matrix from derivatives of Euler angles to angular velocities in the body frame,

$$\mathbf{\Theta} = \begin{bmatrix} 1 & \sin \phi \tan \theta & \cos \phi \tan \theta \\ 0 & \cos \phi & -\sin \phi \\ 0 & \sin \phi \sec \theta & \cos \phi \sec \theta \end{bmatrix}, \quad (17)$$

Note that there are singularities occurring at $\theta = \pm\pi/2$. For the following discussion, we assume that the

movement of the unmanned tandem helicopter does not pass through the singularities.

Equation (16) can be rewritten as

$$\dot{\mathbf{x}} = f(\mathbf{x}) + \sum_{i=1}^4 g_i u_i, \quad (18)$$

where f and g_i are assumed to be smooth vector fields.

3. APPROXIMATE LINEARIZATION BASED DYNAMIC AUGMENT

Select the outputs as

$$\mathbf{y} = h(\mathbf{x}) = [P_x \quad P_y \quad P_z \quad \psi]^T, \quad (19)$$

Pick the j^{th} output y_j and differentiate it with respect to time until encountering one of the inputs. For each output, one can check that the relative degree is 3, i.e.,

$$y_j^{(3)} = L_f^3 h_j + \sum_{i=1}^4 L_{g_i} L_f^2 h_j u_i, \quad (20)$$

So we can rewrite the system as follows,

$$\begin{bmatrix} y_1^{(3)} \\ \vdots \\ y_4^{(3)} \end{bmatrix} = \underbrace{\begin{bmatrix} L_f^3 h_1 \\ \vdots \\ L_f^3 h_4 \end{bmatrix}}_{\mathbf{b}(\mathbf{x})} + \underbrace{\begin{bmatrix} L_{g_1} L_f^2 h_1(\mathbf{x}) & \cdots & L_{g_4} L_f^2 h_1(\mathbf{x}) \\ \vdots & \vdots & \vdots \\ L_{g_1} L_f^2 h_4(\mathbf{x}) & \cdots & L_{g_4} L_f^2 h_4(\mathbf{x}) \end{bmatrix}}_{\mathbf{A}(\mathbf{x})} \begin{bmatrix} u_1 \\ \vdots \\ u_4 \end{bmatrix}, \quad (21)$$

It can be easily verified that $\mathbf{A}(\mathbf{x})$ is invertible in neighborhood \mathbf{U} of equilibrium point \mathbf{x}_0 . So when applying state feedback control law

$$\mathbf{u} = -\mathbf{A}^{-1}(\mathbf{x})\mathbf{b}(\mathbf{x}) + \mathbf{A}^{-1}(\mathbf{x})\mathbf{v}, \quad (22)$$

the input/output dynamic equation can be derived as follows,

$$\begin{bmatrix} y_1^{(3)} \\ \vdots \\ y_4^{(3)} \end{bmatrix} = \begin{bmatrix} v_1 \\ \vdots \\ v_4 \end{bmatrix}. \quad (23)$$

It is a linear state equation, and can be solved by linear control theory. Notice that the vector relative degree of the system is (3,3,3,3), then the sum of Kronecker indices is 12, which is less than 16, the

order of the system. So the zero dynamics of the system should be analyzed in order to constrain all outputs and all derivatives of outputs to zero for all time.

Choose the change of coordinates

$$\begin{aligned} \xi_1^1 &= h_1(\mathbf{x}), \\ \xi_2^1 &= L_f h_1(\mathbf{x}), \\ \xi_3^1 &= L_f^2 h_1(\mathbf{x}), \\ \xi_1^2 &= h_2(\mathbf{x}), \\ \xi_2^2 &= L_f h_2(\mathbf{x}), \\ &\dots \\ \xi_3^4 &= L_f^3 h_4(\mathbf{x}). \end{aligned} \tag{24}$$

So the zero dynamic equation can be parameterized by $\boldsymbol{\eta} = [\phi, p, \theta, q]^T$ with

$$\dot{\boldsymbol{\eta}} = \mathbf{q}(0, \boldsymbol{\eta}), \tag{25}$$

which can be rewritten as

$$\begin{bmatrix} \dot{\phi} \\ \dot{p} \\ \dot{\theta} \\ \dot{q} \end{bmatrix} = \begin{bmatrix} \frac{1}{c\theta}(pc\theta + qs\phi s\theta + rc\phi s\theta) \\ \frac{1}{I_x}(R_m + Y_m^f h_f + Y_m^r h_r - (I_z - I_y)qr) \\ qc\phi - rs\phi \\ \frac{1}{I_y}(M_m - X_m^f h_f - X_m^r h_r) \\ \frac{1}{I_y}(-Z_m^f l_f + Z_m^r l_r - (I_x - I_z)rp) \end{bmatrix} \tag{26}$$

at the equilibrium point of hovering. To linearize it at equilibrium point, the eigenvalues of matrix

$$\frac{\partial \mathbf{q}}{\partial \boldsymbol{\eta}}(0,0), \tag{27}$$

slide on the imaginary axis with different angular velocity r . So the stability property close to the equilibrium can't be determined through zero dynamics.

Let

$$\tilde{\mathbf{P}} = \mathbf{P}/g, \quad \tilde{\mathbf{V}} = \mathbf{v}^p/g, \quad \tilde{T} = T_m/(mg), \tag{28}$$

(11) and (12) can be rewritten as

$$\dot{\tilde{\mathbf{P}}} = \tilde{\mathbf{V}}, \tag{29}$$

$$\tilde{\mathbf{V}} = \mathbf{R}\tilde{\mathbf{F}} + \tilde{\mathbf{g}} + \boldsymbol{\rho}, \tag{30}$$

where

$$\tilde{\mathbf{F}} = \begin{bmatrix} 0 \\ 0 \\ -\tilde{T} \end{bmatrix}, \tag{31}$$

$$\tilde{\mathbf{g}} = \begin{bmatrix} 0 \\ 0 \\ 1 \end{bmatrix}, \tag{32}$$

$$\boldsymbol{\rho} = \mathbf{R} \begin{bmatrix} X_m/(mg) \\ Y_m/(mg) \\ Z_m/(mg) + \tilde{T} \end{bmatrix}. \tag{33}$$

Assume that a_s, b_s^f and b_s^r are small, then $\boldsymbol{\rho}$ is also a small vector that can be ignored. So the system equation can be approximated as

$$\dot{\tilde{\mathbf{x}}} = \begin{bmatrix} \tilde{\mathbf{V}} \\ \mathbf{R}\tilde{\mathbf{F}} + \tilde{\mathbf{g}} \\ \boldsymbol{\Theta}\boldsymbol{\omega}^b \\ \mathbf{I}^{-1}(\boldsymbol{\Gamma} - \boldsymbol{\omega}^b \times \mathbf{I}\boldsymbol{\omega}^b) \\ u_1 \\ u_2 \\ u_3 \\ u_4 \end{bmatrix}, \tag{34}$$

where

$$\tilde{\mathbf{x}} = [\tilde{P}_x, \tilde{P}_y, \tilde{P}_z, \tilde{u}^p, \tilde{v}^p, \tilde{w}^p, \phi, \theta, \psi, p, q, r, \tilde{T}, a_s, b_s^f, b_s^r]^T$$

$$\text{and } \tilde{\mathbf{u}} = [u_1 \ u_2 \ u_3 \ u_4]^T.$$

We select the outputs as

$$\mathbf{y} = h(\tilde{\mathbf{x}}) = [\tilde{P}_x \ \tilde{P}_y \ \tilde{P}_z \ \psi]^T, \tag{35}$$

By the same steps, we can obtain the vector relative degree (3,3,3,3), and the input/output dynamic equation becomes,

$$\begin{bmatrix} h_1^{(3)} \\ h_2^{(3)} \\ h_3^{(3)} \\ h_4^{(3)} \end{bmatrix} = \tilde{\mathbf{b}}(\tilde{\mathbf{x}}) + \underbrace{\begin{bmatrix} L_{g_1} L_f^2 h_1 & 0 & 0 & 0 \\ L_{g_1} L_f^2 h_2 & 0 & 0 & 0 \\ L_{g_1} L_f^2 h_3 & 0 & 0 & 0 \\ L_{g_1} L_f^2 h_4 & L_{g_2} L_f^2 h_4 & L_{g_3} L_f^2 h_4 & L_{g_4} L_f^2 h_4 \end{bmatrix}}_{\tilde{\mathbf{A}}(\tilde{\mathbf{x}})} \begin{bmatrix} u_1 \\ u_2 \\ u_3 \\ u_4 \end{bmatrix} \tag{36}$$

It is obvious that decoupling matrix $\tilde{\mathbf{A}}(\tilde{\mathbf{x}})$ is not full rank. So let

$$z_1 = u_1, \quad \dot{z}_1 = z_2, \quad (37)$$

then

$$\dot{\hat{\mathbf{x}}} = f(\hat{\mathbf{x}}) + g(\hat{\mathbf{x}})\hat{\mathbf{u}}, \quad (38)$$

where

$$\hat{\mathbf{x}} = [\tilde{P}_x, \tilde{P}_y, \tilde{P}_z, \tilde{u}^p, \tilde{v}^p, \tilde{w}^p, \phi, \theta, \psi, p, q, r, \tilde{T}, a_s, b_s^f, b_s^r, z_1]^T$$

and $\hat{\mathbf{u}} = [z_2 \quad u_2 \quad u_3 \quad u_4]^T$.

Differentiating the outputs with the same steps, we get a decoupling matrix $\hat{\mathbf{A}}(\hat{\mathbf{x}})$, which is still not full rank. So let $\dot{z}_2 = v_1$, then the augmented system equation is as follows,

$$\dot{\bar{\mathbf{x}}} = f(\bar{\mathbf{x}}) + g(\bar{\mathbf{x}})\bar{\mathbf{u}}, \quad (39)$$

where

$$\bar{\mathbf{x}} = [\tilde{P}_x, \tilde{P}_y, \tilde{P}_z, \tilde{u}^p, \tilde{v}^p, \tilde{w}^p, \phi, \theta, \psi, p, q, r, \tilde{T}, a_s, b_s^f, b_s^r, z_1, z_2]^T,$$

$$\bar{\mathbf{u}} = [v_1 \quad u_2 \quad u_3 \quad u_4]^T.$$

The input/output dynamic equation eventually becomes,

$$\begin{bmatrix} h_1^{(5)} \\ h_2^{(5)} \\ h_3^{(5)} \\ h_4^{(3)} \end{bmatrix} = \bar{\mathbf{b}}(\bar{\mathbf{x}}) + \underbrace{\begin{bmatrix} L_{g_1} L_f^4 h_1 & L_{g_2} L_f^4 h_1 & L_{g_3} L_f^4 h_1 & L_{g_4} L_f^4 h_1 \\ L_{g_1} L_f^4 h_2 & L_{g_2} L_f^4 h_2 & L_{g_3} L_f^4 h_2 & L_{g_4} L_f^4 h_2 \\ L_{g_1} L_f^4 h_3 & L_{g_2} L_f^4 h_3 & L_{g_3} L_f^4 h_3 & L_{g_4} L_f^4 h_3 \\ L_{g_1} L_f^2 h_4 & L_{g_2} L_f^2 h_4 & L_{g_3} L_f^2 h_4 & L_{g_4} L_f^2 h_4 \end{bmatrix}}_{\bar{\mathbf{A}}(\bar{\mathbf{x}})} \begin{bmatrix} v_1 \\ u_2 \\ u_3 \\ u_4 \end{bmatrix} \quad (40)$$

It can be easily shown that the decoupling matrix $\bar{\mathbf{A}}(\bar{\mathbf{x}})$ is full rank at equilibrium point. The vector relative degree is now (5,5,5,3). Therefore, the sum of Kronecker indices is 18, which is equal to the order of the augmented system.

Define

$$\xi_1^1 = \tilde{P}_x, \quad \xi_1^2 = \tilde{P}_y, \quad \xi_1^3 = \tilde{P}_z, \quad \xi_1^\psi = \psi, \quad (41)$$

then we have

$$\begin{aligned} \dot{\xi}_1^i &= \xi_2^i, & \dot{\xi}_1^\psi &= \xi_2^\psi, \\ \dot{\xi}_2^i &= \xi_3^i + \rho_i(\mathbf{x}), & \dot{\xi}_2^\psi &= \xi_3^\psi, \\ \dot{\xi}_3^i &= \xi_4^i, & \dot{\xi}_3^\psi &= \mathbf{b}^\psi + \mathbf{A}^\psi \mathbf{u}, \\ \dot{\xi}_4^i &= \xi_5^i, \\ \dot{\xi}_5^i &= \mathbf{b}^i + \mathbf{A}^i \mathbf{u}, \end{aligned} \quad (42)$$

where $i=1,2,3$, and $\boldsymbol{\rho}$ is defined in (33).

So we can design the output tracking control law as follows,

$$\mathbf{u} = -\bar{\mathbf{A}}^{-1}(\bar{\mathbf{x}})\bar{\mathbf{b}}(\bar{\mathbf{x}}) + \bar{\mathbf{A}}^{-1} \begin{bmatrix} y_{d1}^{(5)} - \alpha_1^1 e_1^{(4)} - \dots - \alpha_5^1 e_1 \\ y_{d2}^{(5)} - \alpha_1^2 e_2^{(4)} - \dots - \alpha_5^2 e_2 \\ y_{d3}^{(5)} - \alpha_1^3 e_3^{(4)} - \dots - \alpha_5^3 e_3 \\ y_{d4}^{(3)} - \alpha_1^4 e_4^{(2)} - \dots - \alpha_3^4 e_4 \end{bmatrix}, \quad (43)$$

where

$$e_i^{(j)} = \xi_{j+1}^i - y_{di}^{(j)}, \quad i=1,2,3, \quad j=1, \dots, 5$$

and

$$e_4^{(j)} = \xi_{j+1}^4 - y_{d4}^{(j)}, \quad j=1,2,3,$$

the polynomials $s^5 + \alpha_1^i s^4 + \dots + \alpha_5^i, i=1,2,3$ and $s^3 + \alpha_1^4 s^2 + \alpha_2^4 s + \alpha_3^4$ chosen Hurwitz. The states of the system are constrained by the following theorem when applying the control law.

Theorem 1 : Given that the desired trajectory and its first $\gamma_i - 1$ derivatives are bounded, then the states of the transformed system (28) are bounded and the tracking errors satisfy

$$|e_i| = |\xi_1^i - y_{di}| \leq k\varepsilon, \quad i=1, \dots, 4,$$

where

$$\varepsilon = \max(|a_s|, |b_s^f|, |b_s^r|),$$

and k is bounded.

Proof: see appendix.

4. SIMULATION RESULTS

In this section, we present the simulation of the behavior of the complete unmanned tandem helicopter dynamics, and the dynamic augment method used to obtain the control law. The experiment considers the case of stabilization of the unmanned tandem helicopter dynamics to a hovering configuration. The following parameters are for our unmanned tandem helicopter:

$m = 46\text{kg}$	$g = 9.8\text{m/s}^2$	$I_x = 1.5\text{kg} \cdot \text{m}^2$
$I_y = 2.9\text{kg} \cdot \text{m}^2$	$I_z = 3.0\text{kg} \cdot \text{m}^2$	$l_f = 0.98\text{m}$
$l_r = 0.90\text{m}$	$h_f = 0.30\text{m}$	$h_r = 0.45\text{m}$
$k_1 = 0.005$	$k_2 = 0.7$	$\alpha_f = 25$
$\alpha_r = -25$	$\beta_f = 25$	$\beta_r = -25$
$\rho_f = k_1 T_f^{1.5} + k_2$	$\rho_r = -k_1 T_r^{1.5} - k_2$	$c_1 = 5.35$
$c_3 = 74.28$		

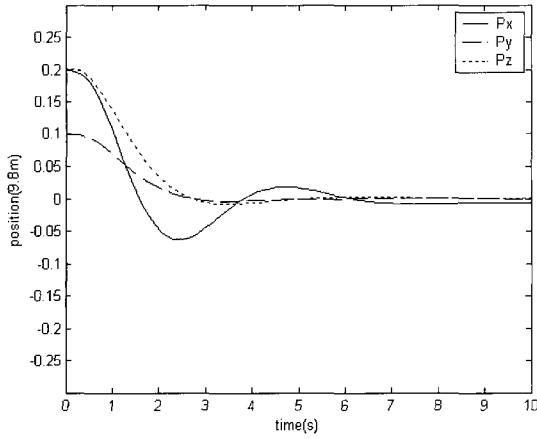


Fig. 3. The position outputs.

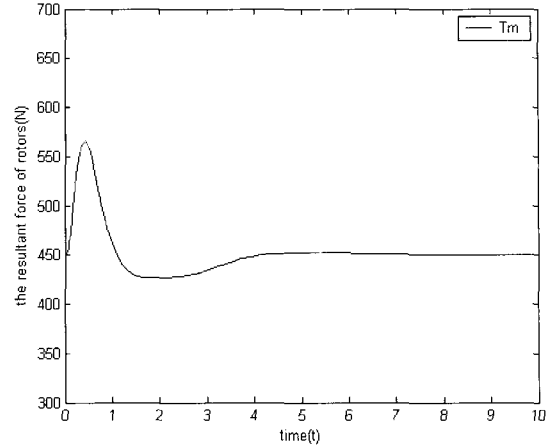


Fig. 5. The resultant thrust force of rotors.

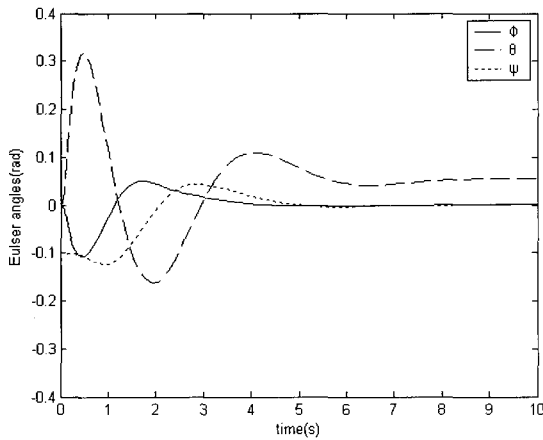


Fig. 4. The Euler angles outputs.

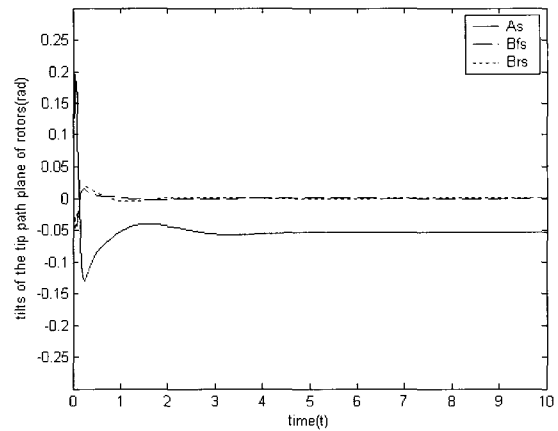


Fig. 6. The tilts of the tip path plane of rotors.

Figs. 3 and 4 display the position and attitude of the unmanned tandem helicopter. There exists a steady state error in the longitudinal position, which is brought here because of approximation. The error is constrained by theorem 1, and it is acceptable. The thrust force and tilt of the rotor's tip path are shown in Figs. 5 and 6, and they are kept in reasonable bound throughout the simulation. The internal dynamics are stabilized by applying the approximate control law.

5. CONCLUSIONS

In this paper, we have derived a simple mathematical model for an unmanned tandem helicopter, and developed an approach to track the output of the helicopter near hovering, which is based on the dynamic augment method. Simulation results show that the control law produces desired performance within the bounded error. In future work, we will implement the controller on an unmanned tandem helicopter developed by our team.

APPENDIX A: PROOF OF THEOREM 1

The system can be rewritten as follows,

$$\begin{aligned}
 \dot{\zeta}_1^i &= \zeta_2^i & \dot{\zeta}_1^\psi &= \zeta_2^\psi \\
 \dot{\zeta}_2^i &= \zeta_3^i + \rho_i(x) & \dot{\zeta}_2^\psi &= \zeta_3^\psi \\
 \dot{\zeta}_3^i &= \zeta_4^i & \dot{\zeta}_5^\psi &= \mathbf{b}^\psi + \mathbf{A}^\psi \mathbf{u} \\
 \dot{\zeta}_4^i &= \zeta_5^i & & \\
 \dot{\zeta}_5^i &= \mathbf{b}^i + \mathbf{A}^i \mathbf{u} & &
 \end{aligned} \tag{A.1}$$

where $i = 1, 2, 3$.

Without loss of generality, we select $i = 1$, then from (33)

$$\boldsymbol{\rho} = \mathbf{R} \begin{bmatrix} X_m / (mg) \\ Y_m / (mg) \\ Z_m / (mg) + \tilde{T} \end{bmatrix}, \tag{A.2}$$

we have

$$\begin{aligned}
 \rho_1 &= R_{11} X_m / (mg) + R_{12} Y_m / (mg) \\
 &\quad + R_{13} (Z_m / (mg) + \tilde{T}), \tag{A.3}
 \end{aligned}$$

it can be rewritten as

$$\begin{aligned}
 \rho_1 &= -R_{11}\tilde{T} \sin a_s + R_{12}\tilde{T}(\sin b_s^f + \sin b_s^r) \\
 &\quad - R_{13}\tilde{T} \cos a_s (\cos b_s^f + \cos b_s^r) \\
 &= -\cos \psi \cos \theta \tilde{T} \sin a_s + (-\sin \psi \cos \phi \\
 &\quad + \cos \psi \sin \theta \sin \phi) \tilde{T} (\sin b_s^f + \sin b_s^r) \\
 &\quad - (\sin \psi \sin \phi + \cos \psi \sin \theta \cos \phi) \tilde{T} \\
 &\quad \cdot (\cos a_s (\cos b_s^f + \cos b_s^r) - 2) \\
 &\leq \tilde{T} (|\cos \psi \cos \theta \sin a_s| + (|\sin \psi \cos \phi| \\
 &\quad + |\cos \psi \sin \theta \sin \phi|) (|\sin b_s^f| + |\sin b_s^r|) \\
 &\quad + (|\sin \psi \sin \phi| + |\cos \psi \sin \theta \cos \phi|) \\
 &\quad \cdot (|\cos a_s (\cos b_s^f + \cos b_s^r) - 2|)) \\
 &\leq \tilde{T} (|a_s| + |\psi| |b_s^f| + |\theta \phi| |b_s^f| + |\psi| |b_s^r| \\
 &\quad + |\theta \phi| |b_s^r| + 2(|\psi \phi| + |\theta|) |a_s|)
 \end{aligned} \tag{A.4}$$

let

$$\varepsilon = \max (|a_s|, |b_s^f|, |b_s^r|) \tag{A.5}$$

then

$$\begin{aligned}
 \rho_1 &\leq \tilde{T} (|a_s|/\varepsilon + |\psi| |b_s^f|/\varepsilon + |\theta \phi| |b_s^f|/\varepsilon + |\psi| |b_s^r|/\varepsilon \\
 &\quad + |\theta \phi| |b_s^r|/\varepsilon + 2(|\psi \phi| + |\theta|) |a_s|/\varepsilon) \varepsilon \\
 &\leq \varepsilon \tilde{T} (1 + |\psi| + |\theta \phi| + |\psi| + |\theta \phi| + 2(|\psi \phi| + |\theta|)) \tag{A.6} \\
 &= \varepsilon \tilde{T} (1 + 2|\psi| + 2|\theta \phi| + 2|\psi \phi| + 2|\theta|) \\
 &\leq \varepsilon K \tilde{T},
 \end{aligned}$$

Define error vector

$$\mathbf{e} = [e_1 \quad \dots \quad e_5] \tag{A.7}$$

where

$$e_i = \xi_i^1 - y_{di}^{(i-1)}, \quad i = 1, \dots, 5. \tag{A.8}$$

Then we have

$$\begin{bmatrix} \dot{e}_1 \\ \dot{e}_2 \\ \dot{e}_3 \\ \dot{e}_4 \\ \dot{e}_5 \end{bmatrix} = \underbrace{\begin{bmatrix} 0 & 1 & \dots & 0 \\ \vdots & 0 & \ddots & \vdots \\ 0 & \dots & 0 & 1 \\ -\alpha_0 & -\alpha_1 & \dots & -\alpha_4 \end{bmatrix}}_{\mathbf{A}} \begin{bmatrix} e_1 \\ e_2 \\ e_3 \\ e_4 \\ e_5 \end{bmatrix} + \begin{bmatrix} 0 \\ \rho_1 \\ 0 \\ 0 \\ 0 \end{bmatrix}. \tag{A.9}$$

Consider the Lyapunov function for above error system as follows,

$$\mathbf{V} = \mathbf{e}^T \mathbf{P} \mathbf{e}, \tag{A.10}$$

where \mathbf{P} is a positive symmetrical matrix that satisfies

$$\mathbf{A}^T \mathbf{P} + \mathbf{P} \mathbf{A} = -\mathbf{I}. \tag{A.11}$$

Reflecting on the derivative of \mathbf{V} , we have

$$\begin{aligned}
 \dot{\mathbf{V}} &= \dot{\mathbf{e}}^T \mathbf{P} \mathbf{e} + \mathbf{e}^T \mathbf{P} \dot{\mathbf{e}} \\
 &= 2\mathbf{b}^T \mathbf{P} \mathbf{e} - \mathbf{e}^T \mathbf{e} \\
 &\leq -\|\mathbf{e}\|^2 + 2K\varepsilon \|\mathbf{P}\| \|\mathbf{e}\|.
 \end{aligned} \tag{A.12}$$

since \mathbf{P} is a positive and symmetrical matrix, so it can be represented as

$$\mathbf{P} = \mathbf{U}^T \begin{bmatrix} a_1 & & 0 \\ & \ddots & \\ 0 & & a_5 \end{bmatrix} \mathbf{U}, \tag{A.13}$$

where a_i is the eigenvalue of \mathbf{P} , and $|\mathbf{U}| = 1$.

Assume that λ_i is the eigenvalue of \mathbf{A} , then we have

$$a_i \mathbf{x} = \mathbf{P} \mathbf{x}, \tag{A.14}$$

$$\lambda_i \mathbf{x} = \mathbf{A} \mathbf{x}, \tag{A.15}$$

while

$$\mathbf{x}^T \mathbf{A}^T \mathbf{P} \mathbf{x} + \mathbf{x}^T \mathbf{P} \mathbf{A} \mathbf{x} = -\mathbf{x}^T \mathbf{x}, \tag{A.16}$$

so

$$2\lambda_i \mathbf{x}^T \mathbf{P} \mathbf{x} = -\mathbf{x}^T \mathbf{x}, \tag{A.17}$$

which derives

$$2\lambda_i \mathbf{x}^T a_i \mathbf{x} = -\mathbf{x}^T \mathbf{x}, \tag{A.18}$$

we get

$$a_i = -1/(2\lambda_i). \tag{A.19}$$

We can let $\lambda_i < -1$ through pole assignment, then $0 < a_i < 1/2$. So we have

$$\begin{aligned}
 \dot{\mathbf{V}} &\leq -\|\mathbf{e}\|^2 + 2K\varepsilon \|\mathbf{P}\| \|\mathbf{e}\| \\
 &\leq -\|\mathbf{e}\|^2 + 2K\varepsilon (\max a_i)^5 \|\mathbf{e}\| \\
 &\leq -\|\mathbf{e}\|^2 + K\varepsilon \|\mathbf{e}\|,
 \end{aligned} \tag{A.20}$$

If $\|\mathbf{e}\| > \varepsilon K$, then $\dot{\mathbf{V}} < 0$, and the error trend is toward zero. If $\|\mathbf{e}\| \leq \varepsilon K$, it is obvious that the error is bounded by a positive number εK . So we can conclude that the tracking error is bounded. \square

REFERENCES

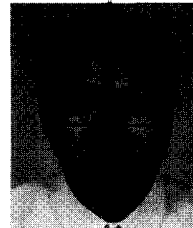
- [1] B. A. Kenneth and J. T. Robert, "Studies of the lateral-directional flying qualities of a tandem helicopter in forward flight," *NACA Rep. 1207*, pp. 1159-1173, 1953.
- [2] J. T. Robert and B. A. Kenneth, "Studies of the speed stability of a tandem helicopter in forward flight," *NACA Rep. 1260*, pp. 201-212, 1953.

- [3] J. E. Yeates, "Flight measurements of the vibration experienced by a tandem helicopter in transition, vortex-ring state, landing approach, and tawed flight," *NACA Technical Note 4409*, pp. 1-20, 1958.
- [4] B. Sridhar and P. Lindorff, "Application of poplacement theory to helicopter stabilization systems," *Proc. of the 6th Hawaii International Conference on Systems Sciences*, pp. 405-407, 1973.
- [5] R. F. Stengel, J. R. Broussard, and P. W. Berry, "Digital flight control design for a tandem-rotor helicopter," *Automatica*, vol. 14, no. 4, pp. 301-312, 1978.
- [6] C.-Y. Huang, R. Celi, and I.-C. Shih, "Reconfigurable flight control systems for a tandem rotor helicopter," *Journal of the American Helicopter Society*, vol. 44, no. 1, pp. 50-62, 1999.
- [7] Dzul and T. Hamel, "Nonlinear control for a tandem rotor helicopter," *15th Triennial World Congress*, pp. 21-26, 2002.
- [8] T. J. Koo and S. Sastry, "Output tracking control design of a helicopter model based on approximate linearization," *Proc. of the 37th IEEE Conference on Decision & Control*, pp. 3635-3640, 1998.
- [9] G. Meyer, R. Su, and L. R. Hunt, "Application of nonlinear transformation to automatic flight control," *Automatica*, vol. 20, no. 1, pp. 103-107, 1984.
- [10] H. Shim, T. J. Koo, F. Hoffmann, and S. Sastry, "A comprehensive study of control design for an autonomous helicopter," *Proc. of the 37th IEEE Conference on Decision & Control*, pp. 3635-3640, 1998.
- [11] Y. Ma, "A differential geometric approach to computer vision and its applications in control," *Ph. D. thesis*, UC Berkeley, August 2000.



and automated UAVs.

Chun-Hua Hu received his B.S. degree in Computer Science and Technology from Tsinghua University, China, in 1999. He is currently a candidate for a Ph.D. degree in the Department of Computer Science and Technology, Tsinghua University. His research interests are in the areas of nonlinear control, intelligent control



Section, and a Council Member of the Chinese Association of Automation.

Zeng-Qi Sun is the author and/or co-author of over 200 papers and seven books on intelligent control and robotics. His current research interests include intelligent control, robotics, fuzzy systems, neural networks and evolution computing, etc.

Zeng-Qi Sun (SM'93) received the Ph.D. degree in Control Engineering in 1981 from the Chalmers University of Technology in Sweden.

He is currently a Professor in the Department of Computer Science and Technology, Tsinghua University, China. He is also Senior Member of IEEE, an Executive Member of IEEE's Beijing